



Water soluble binder for fabrication of $\text{Li}_4\text{Ti}_5\text{O}_{12}$ electrodes

Elina Pohjalainen^a, Samuli Räsänen^b, Miikka Jokinen^a, Kirsi Yliniemi^{a,c}, David A. Worsley^c, Juha Kuusivaara^d, Jouni Juurikivi^e, Risto Ekqvist^f, Tanja Kallio^{a,*}, Maarit Karppinen^a

^a Department of Chemistry, School of Chemical Technology, Aalto University, P.O. Box 16100, FI-00076 Aalto, Finland

^b Kokkola University Consortium Chydenius, Department of Chemistry, P.O. Box 567, FI-67701 Kokkola, Finland

^c SPECIFIC, Swansea University, Baglan Bay Innovation & Knowledge Centre, Unit 20 Central Avenue, Baglan Energy Park, Baglan, Port Talbot SA12 7AX, United Kingdom

^d Sachtleben Pigments Oy, Titaanitie, FI-28840 Pori, Finland

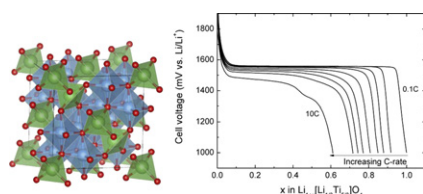
^e Sun Chemical Oy, Pieni teollisuuskatu 2, FI-02920 Espoo, Finland

^f Walki Oy, Luodontie 151, FI-68600 Pietarsaari, Finland

HIGHLIGHTS

- Acryl S020 binder is introduced for aqueous electrode preparation process.
- Acryl $\text{Li}_4\text{Ti}_5\text{O}_{12}$ electrodes show good capacity retention up to a rate of 10 C.
- Acryl $\text{Li}_4\text{Ti}_5\text{O}_{12}$ electrodes show reversible capacity loss at sub-zero temperatures.
- Cycle life of 500 is obtained with electrodes prepared in aqueous pilot-scale process.

GRAPHICAL ABSTRACT



ARTICLE INFO

Article history:

Received 11 July 2012

Received in revised form

28 September 2012

Accepted 29 October 2012

Available online 8 November 2012

Keywords:

Li-ion battery

Lithium titanate

Acrylate

Aqueous electrode preparation process

ABSTRACT

Less expensive and greener aqueous electrode preparation processes are essential for the market penetration of lithium ion batteries to mid-scale applications. So far only carboxyl methyl cellulose (CMC) binder has been adopted for industrial use to fabricate carbon electrodes without harmful organic solvents but this process is prone to bacterial growth.

In this study a new binder candidate, Acryl S020, is introduced for an aqueous preparation process that has been used for preparing $\text{Li}_4\text{Ti}_5\text{O}_{12}$ electrodes for lithium ion batteries. It is shown that with our water based process electrodes with capacities comparable to those electrodes fabricated with the conventional organic solvent based process with the PVDF binder are obtained. Moreover, our lithium titanate electrodes with the Acryl S020 binder show high capacity retention and they can be operated at sub-zero temperatures. Electrodes were also fabricated with pilot-scale gravure printing and slot-die coating methods and they showed stable cycles lives of 500 cycles.

© 2012 Elsevier B.V. Open access under [CC BY license](http://creativecommons.org/licenses/by/3.0/).

1. Introduction

Development of safe, inexpensive and durable lithium ion batteries that can operate at wide temperature ranges is essential to successfully corner the markets in vehicle and other mid-scale

applications of batteries. However, currently electrodes in the commercial lithium ion batteries are mostly fabricated using harmful and expensive organic solvents such as *N*-methyl-2-pyrrolidone (NMP) and thus, new materials and fabrication processes are needed. Moreover, polyvinylidene fluoride (PVDF) used most commonly as a binder is relatively expensive and environmentally unfriendly as it requires the use of NMP and is not easily disposable in the end of the battery life. Moreover, in the case of graphite negative electrode, safety issues have been raised up

* Corresponding author. Tel.: +358 50 5637 567; fax: +358 9 470 22580.
E-mail address: tanja.kallio@aalto.fi (T. Kallio).

concerning the possible side reactions between PVDF and lithiated graphite under extreme conditions [1]. Therefore, water-based processes are currently investigated intensively to replace the methodology built on utilization of organic solvents with more affordable and environmentally benign aqueous fabrication processes. Water-soluble binders have been introduced for fabrication of LiCoO_2 [2–4], LiFePO_4 [5–10], graphite [8,11–15], and $\text{Li}_4\text{Ti}_5\text{O}_{12}$ [10] electrodes.

The main challenge in the development of water-based electrode fabrication processes is to find an appropriate binder without sacrificing the performance of the whole battery. This is a demanding task as the binder affects, besides the electrode properties, also the whole fabrication process and thus, so far only carboxyl methyl cellulose (CMC) binder has been accepted for industrial use to fabricate carbon electrodes. Actually, to our knowledge, it is the only water-soluble binder reported for $\text{Li}_4\text{Ti}_5\text{O}_{12}$ electrodes. By using water soluble CMC binder, electrodes with lower binder content [16] and higher compactness [7] have been obtained when compared to electrodes fabricated with the PVDF binder. However, CMC is prone to bacterial growth and there is an apparent chase for other water-soluble binder candidates.

The purpose of this paper is to introduce an aqueous electrode fabrication process utilizing an Acryl S020 binder for preparing $\text{Li}_4\text{Ti}_5\text{O}_{12}$ electrodes. Acrylates have been used as binders in paints and varnishes since 1950s and nowadays increasingly in packaging finishes. Thus, acrylates with a variety of well-known properties are commercially available in reasonable price and therefore, they are interesting candidates for aqueous electrode fabrication processes for lithium ion batteries.

Lithium titanate, $\text{Li}_4\text{Ti}_5\text{O}_{12}$, is an alternative negative electrode material to the conventionally used graphite and it has been studied since the beginning of 1990's and commercialized a few years ago. It is a zero-strain-material *i.e.* only small changes in lattice dimensions during charging and discharging are observed and thus it would be an ideal counterpart for lithium iron phosphate, LiFePO_4 , a positive electrode material showing also small dimensional changes upon cycling. Environmentally friendly and inexpensive lithium titanate has a long cycle life and additionally, it is tolerant against abuse. Unlike graphite, it can also be charged at sub-zero temperatures and, because of high lithium insertion potential (1.55 V vs. Li/Li^+), no formation of solid electrolyte interphase (SEI) takes place and thus, a high-rate charging is possible. As a summary, $\text{Li}_4\text{Ti}_5\text{O}_{12}$ is a promising negative electrode material for safe batteries which could be operated at a wide temperature range and show a long life time.

Here, the performance of lithium titanate electrodes fabricated with the Acryl S020 binder in an aqueous solution is demonstrated at various C-rates and at sub-zero temperatures: the performance is also compared to the electrodes prepared by organic solvent based process using PVDF as a binder. Moreover, the electrode fabrication process is also transferred from the laboratory scale to the pilot line scale: the electrodes are prepared both by pilot-scale gravure printing and slot die coating methods and the performance of the batteries constructed of these types of electrodes is investigated.

2. Experimental

2.1. Laboratory-scale electrode preparation

Commercial single-phase $\text{Li}_4\text{Ti}_5\text{O}_{12}$ powder (Sachtleben Pigments) with specific surface area of $50 \text{ m}^2 \text{ g}^{-1}$ and particle size of 250 nm was used as an active electrode material. In the electrode manufacturing process carbon black (Super P, Timcal) was used as a conductive additive and PVDF (polyvinylidene fluoride, Kureha) or Acryl S020 (Sun Chemical) was used as a binder. PVDF was

dissolved in NMP (*N*-methyl-2-pyrrolidone; Emplura®, Merck) and Acryl S020 was dissolved in deionized water. The starting materials for the electrode slurry, used in the mass ratio of 86:8:6 for $\text{Li}_4\text{Ti}_5\text{O}_{12}$:binder:carbon black, were added in the solvent in the order of binder, lithium titanate and carbon black, and mixed using a dispergator (VMA-Getzmann GMBH Dispermat CV) at 6000–8000 rpm speed until the slurry was homogeneous. The slurry was coated manually on aluminium foil and the coated foils were dried at 130 °C for 24 h.

2.2. Pilot-scale electrode fabrication processes

Two methods resulting in different amounts of active material on the aluminium foil acting as a current collector and a substrate were selected for fabrication of the electrodes in pilot scale, namely gravure printing and slot die coating methods.

Gravure method was selected for pilot-scale electrode preparation as a mechanically simple and direct high quality printing process. A Pagendam TKW dispersion machine was used for the experiments. The gravure process employed a metal printing cylinder onto which the image was etched while the ink was transferred directly to the substrate from small cells that were precisely engraved into the surface of the printing cylinder (image carrier). These engraved cells were filled by rotating the cylinder in an ink pan while the excess ink was wiped from the printing cylinder surface by a doctor blade as the cylinder turned past the blade. The substrate, *i.e.* aluminium foil, was pressed onto the printing cylinder surface by a rubber covered impression roller resulting in a direct ink transfer on the substrate.

Slot die, another method selected for the pilot-scale electrode preparation, is a coating technology capable of high production speed with good coating uniformity. In the slot die process coating slurry was supplied to the die at constant speed by a precision pump and applied through a slot onto the moving substrate (aluminium foil) supported on a roller using a Meltex EPS 1-2 apparatus. All the coating slurry fed into the die was applied on the substrate eliminating the need to recirculate the slurry and thus resulting in a good waste management and reduced contaminations. Other advantages of slot die coating method included high and uniform quality of the coating, and good and efficient control over the coating weight.

The electrode slurries were mixed by Sun Chemical using a VMA dispermat dispergator and printing/coating was conducted by Walki Group. After preparing the lithium titanate electrodes, pieces with 8 mm diameter were cut from the coated aluminium foil and let to dry in the glove box for 7 day before assembling the half-cells. The half-cells of the batteries were assembled with exactly same procedure when using either the laboratory-scale and pilot-scale prepared electrodes.

2.3. Humidity-TG measurements

Thermogravimetric (TG) measurements were performed to find out how water affects the lithium titanate during the preparation process. The water absorption/desorption process was investigated *in-situ* using a humidity-TG device, which consisted of a source of compressed air (AGA; 79.1% N_2 , 20.9% O_2), a humidifier, a gas-controller unit (Perkin–Elmer Thermal Analysis Gas Station), a thermobalance (Perkin–Elmer Pyris 1 TGA HT), an N_2 gas source, and a humidity analyser (Vaisala DMP248). The device is described in detail elsewhere [17,18].

The TG heating program included 5 steps starting with (i) isothermal heating in dry air (relative humidity 1.8%) at 130 °C for 2 h, followed by (ii) cooling to 30 °C in dry air *plus* stabilization period of 2 h, (iii) switching to humid atmosphere (relative

humidity 35%) at 30 °C for 2 h, (iv) switching to dry air at 30 °C for 2 h, and (v) heating up to 130 °C for 2 h.

2.4. AFM – SKP imaging

Atomic Force Microscope – Scanning Kelvin Probe (AFM – SKP, JPK Instruments, NanoWizard 3 with Si tips for force modulation, Nanoworld) was used to characterise the $\text{Li}_4\text{Ti}_5\text{O}_{12}$ electrodes with the PVDF and Acryl S020 binder. Topographic imaging was performed at the tapping mode during the forward line scan and the potential maps were detected using the SKP mode of the instrument during the reverse line scan. The scanning area was $5 \times 5 \mu\text{m}$, the line frequency 0.5 Hz and the tip potential varied between 0.50 and 0.60 V. The tip was hovering at a constant height (50 nm) above the surface during the SKP scan (reverse line scan).

2.5. Electrochemical tests

Electrochemical testing was conducted with standard 2032-type coin cells. Circular lithium titanate working electrodes of 8 mm in diameter were cut from the electrode foil and calendered with the pressure of 2000 kg cm^{-2} . Lithium metal foil (0.38 mm thick, Aldrich) was used as a counter electrode and 1 M LiPF_6 in ethylene carbonate:dimethyl carbonate 1:1 w/w (LP 30®, Merck) as an electrolyte. 25 μm thick porous polymer membrane (Celgard 2300) or 260 μm thick glass microfiber filter (GF/A, Whatman) was used as a separator. Coin cells were assembled in an argon filled glove box with oxygen and water vapour levels below 1 ppm.

Charging/discharging experiments were done by Neware battery cycler. Galvanostatic charging and discharging was done between 1.0 V and 3.0 V vs. Li/Li^+ at C-rates from 0.1 C to 10 C (1 C corresponds to charging or discharging in 1 h with theoretical capacity of 175 mAh g^{-1}). At least three different coin cells were assembled and measured for each electrode sample.

Electrochemical impedance spectroscopy (EIS) was conducted with Autolab potentiostat (PGSTAT302N) using Nova software. Frequency range was set from 500 kHz to 0.1 Hz and alternating current amplitude was 0.01 mA. EIS data were collected at 75% state of the charge (SOC) at 20 °C, 10 °C, 0 °C and –10 °C. Temperatures below room temperature were reached using a Haake A 24B cryostat for cooling. Each temperature was let to stabilize for 1 h before the EIS measurement.

3. Results and discussion

Applicability of an aqueous electrode preparation process may be limited by the structural instability and the reactivity of an electrode material in water. In order to investigate the durability of $\text{Li}_4\text{Ti}_5\text{O}_{12}$ in water/humid atmosphere, measurements with a humidity-TG device have been carried out to follow the water absorption and desorption behaviour of the electrode materials *in-situ* and in a highly sensitive manner under precisely controlled relative humidity levels [17,18]. Fig. 1 displays TG curves recorded for the $\text{Li}_4\text{Ti}_5\text{O}_{12}$ powder. At first (Step i) the sample is annealed at 130 °C in dry air (relative humidity 1.8%) for 2 h to remove the water absorbed in the sample *prior* to the experiment: a clear flattening of the mass curve is observed during this step confirming that the 2-hour annealing period is long enough to remove any absorbed water from the sample. In following step (Step ii) the sample is cooled down to 30 °C in dry air. Here the $\text{Li}_4\text{Ti}_5\text{O}_{12}$ powder behaves similarly to LiFePO_4 [17], i.e. it absorbs water even in dry air; the difference is that the amount of absorbed water is nearly 20 times larger in the case of $\text{Li}_4\text{Ti}_5\text{O}_{12}$ (~9000 ppm; Fig. 1) than in the case of the LiFePO_4 powder (~500 ppm [17]). This difference cannot be explained solely by the dissimilar surface areas as it is only less than

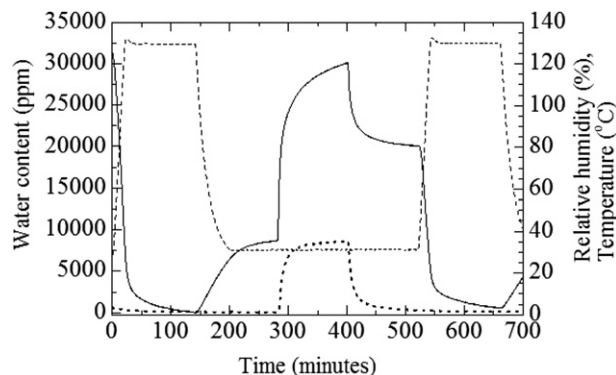


Fig. 1. In-situ water absorption/desorption TG curve for $\text{Li}_4\text{Ti}_5\text{O}_{12}$ powder (solid line), temperature (upper dashed line) and relative humidity (lower dashed line).

5 times larger for the $\text{Li}_4\text{Ti}_5\text{O}_{12}$ powder than for the LiFePO_4 powder. Instead, this suggests a bulk-type absorption for the major part of the water intake for $\text{Li}_4\text{Ti}_5\text{O}_{12}$. Upon increasing the humidity level to 35% in Step iii the water content of the $\text{Li}_4\text{Ti}_5\text{O}_{12}$ powder jumps up to ~30000 ppm very rapidly (Fig. 1). Then once the relative humidity level is lowered back to the 1.8% level in Step iv, the amount of absorbed water clearly decreases but not down to the zero level yet. We assign the part of the absorbed water that follows the surrounding humidity level to surface-adsorbed water. The final heating Step v in dry air at 130 °C drops the water level close to the zero level, showing that the water absorption/desorption process is nearly reversible with the parameters used in the experiment. It should be noted here that the drying temperature for $\text{Li}_4\text{Ti}_5\text{O}_{12}$ electrodes is also 130 °C which is shown here to be enough to remove water from $\text{Li}_4\text{Ti}_5\text{O}_{12}$.

It is well-known that the lithium ion batteries are sensitive to humidity because of HF formation of the LiPF_6 salt in contact with water. So the above-described fast uptake of water even in dry air should be kept in mind when assembling batteries using $\text{Li}_4\text{Ti}_5\text{O}_{12}$ as it may be harmful for the operation of the electrochemical cell, even if titanium is not oxidized beyond the tetravalent state suggesting that $\text{Li}_4\text{Ti}_5\text{O}_{12}$ itself should not be affected by the absorbed water. However, the absorbed water is readily removed by heating $\text{Li}_4\text{Ti}_5\text{O}_{12}$ as the water absorption/desorption process is reversible as shown in Fig. 1 and consequently, batteries free from harmful water can be constructed with lithium titanate electrodes fabricated using an aqueous process.

The effect of the two different binders (PVDF and Acryl S020) on the electrode morphology has been studied by atomic force microscopy – scanning Kelvin probe (AFM – SKP) and Fig. 2 shows AFM – SKP images of the $\text{Li}_4\text{Ti}_5\text{O}_{12}$ electrodes with both binders. From the topographic images (Fig. 2a and b) it can be clearly seen that Acryl S020 creates larger agglomerates on the surface while PVDF bounds the $\text{Li}_4\text{Ti}_5\text{O}_{12}$ to the surface in a more homogeneous manner. However, the potential difference inside the agglomerates produced with the Acryl S020 binder (e.g. white circles in Fig. 2b and d) suggests that the agglomerates themselves consist of separate areas of the binder and the titanate creating several small titanate areas exposed. Therefore, these electrodes—fabricated with an aqueous process—could compete in performance as an active electrode in the Li-ion batteries with the electrodes prepared with a PVDF binder and an organic solvent based process.

To investigate this fact further, the performances of the electrodes prepared either by an aqueous or organic solvent based process (and with the two different binders, Acryl S020 and PVDF, respectively) were compared by studying the charge discharge behaviour of the cells at rates of 0.1 C, 0.2 C, 0.5 C, 1 C, 2 C, 3 C, 4 C,

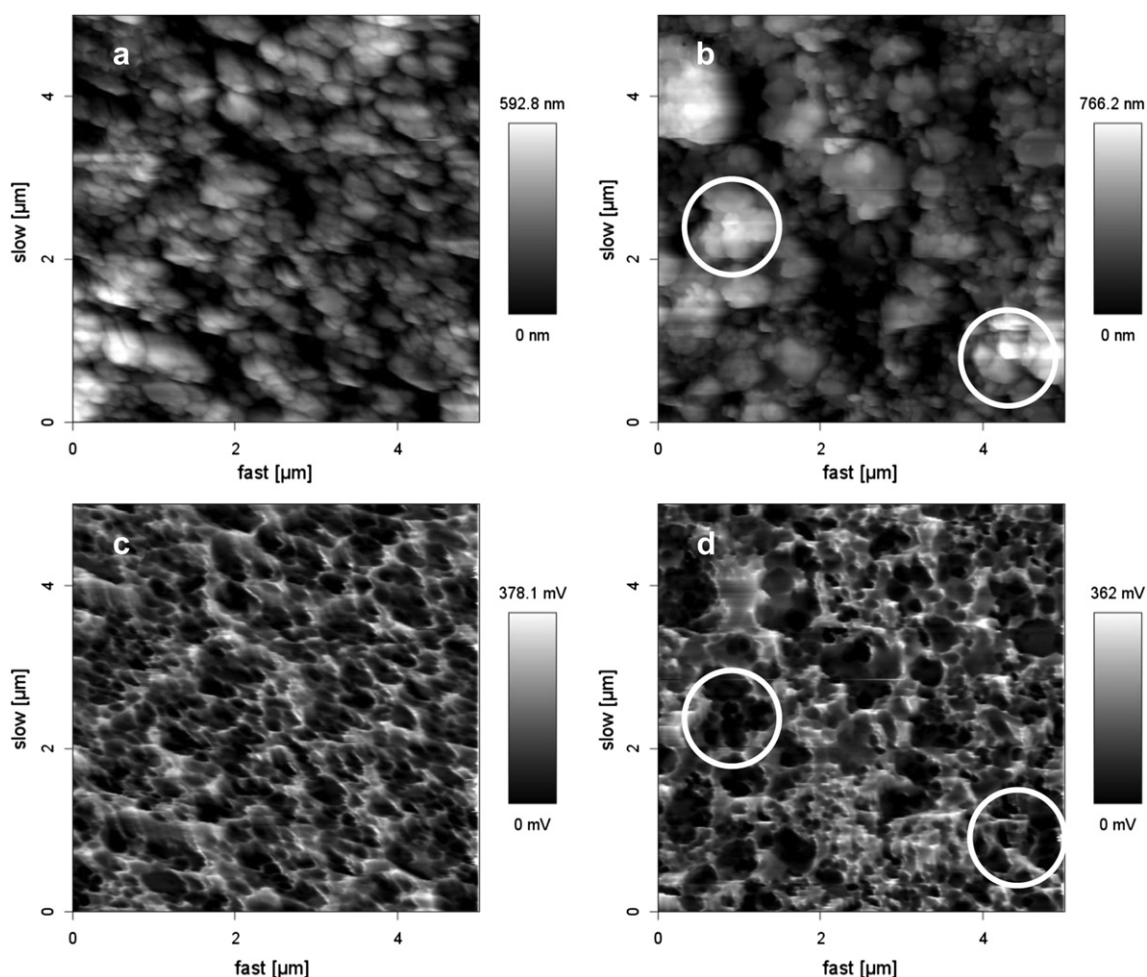


Fig. 2. AFM images of $\text{Li}_4\text{Ti}_5\text{O}_{12}$ electrodes with a) PVDF and b) Acryl S020 binder and potential maps of $\text{Li}_4\text{Ti}_5\text{O}_{12}$ electrodes with c) PVDF and d) Acryl S020 binder.

5 C and 10 C. Typical specific discharge capacities of half cells with the $\text{Li}_4\text{Ti}_5\text{O}_{12}$ electrodes and the PVDF and Acryl S020 binder are obtained and they are shown in Fig. 3. Despite the morphological differences shown in the AFM images, similar capacities can be obtained with both the binders at room temperature. Specific capacities obtained at 0.1 C are equal to the maximal theoretical capacity of lithium titanate (175 mAh g^{-1}) within the experimental error, which originates primarily from the low masses of the electrodes (calculated error of specific capacity is approximately $\pm 20 \text{ mAh g}^{-1}$ at 0.1 C and $\pm 10 \text{ mAh g}^{-1}$ at 10 C based on the measurement accuracy of the active material mass). These similar capacities are expected as thicknesses of the $\text{Li}_4\text{Ti}_5\text{O}_{12}$ electrodes with the PVDF and Acryl S020 binder are roughly the same with less than $2 \mu\text{m}$ difference resulting in comparable densities of approximately 2.5 g cm^{-3} . Reversible capacity loss of 39% at the rate of 10 C compared to capacity measured with 0.1 C is observed indicating that the electrode made of the Acryl S020 and $\text{Li}_4\text{Ti}_5\text{O}_{12}$ material has a potential to be used in high power applications.

To compare the $\text{Li}_4\text{Ti}_5\text{O}_{12}$ electrodes with the Acryl S020 and PVDF binder in more detail, the impedance response of the half cells of the aforementioned electrodes has been measured at 20°C . Both the half cells generated similar impedance spectra and typical Nyquist plots are presented in Fig. 4a showing depressed semicircle at high and mid-frequencies representing electrode–electrolyte interfacial processes and low frequency Warburg tail representing diffusion processes [19,20]. Applicability of the Acryl S020 binder

for sub-zero temperatures has been further investigated by measuring impedance of the half cells in the temperatures range of $20 \dots -10^\circ\text{C}$ (Fig. 4b). The ohmic resistance of the half-cell *i.e.* the intersection of the impedance curve with the abscissa at high frequencies increases with decreasing temperature. This increase from 4Ω to 19Ω is accounted mainly for the increased resistance of the ethylene carbonate containing electrolyte at low temperatures. Moreover, as the temperature decreases the diameter of the half-circuit in the Nyquist plots increases indicating that the electrochemical processes become more sluggish. The increase of the ohmic impedance at high frequencies is relatively small compared to the increase in the diameter of the mid-frequency half circuit suggesting that interfacial processes at the electrode–electrolyte interface are the main contributors to the increase of the cell impedance at low temperatures [21]. The capacity loss observed at the lower temperatures is reversible suggesting that no structural or chemical changes have taken place in the electrodes and consequently, the Acryl S020 binder appears to be suitable for batteries operating at sub-zero temperatures. Further characterization is, however, needed in order to find out the long term durability of the $\text{Li}_4\text{Ti}_5\text{O}_{12}$ electrodes with Acryl S020 binder at sub-zero temperatures.

To investigate long term stability of the $\text{Li}_4\text{Ti}_5\text{O}_{12}$ electrodes with the Acryl S020 and PVDF binders, 200 charge/discharge cycles have been measured with the half cells at the rate of 1 C. As shown in Fig. 5, specific capacities (approximately 150 mAh g^{-1} for the

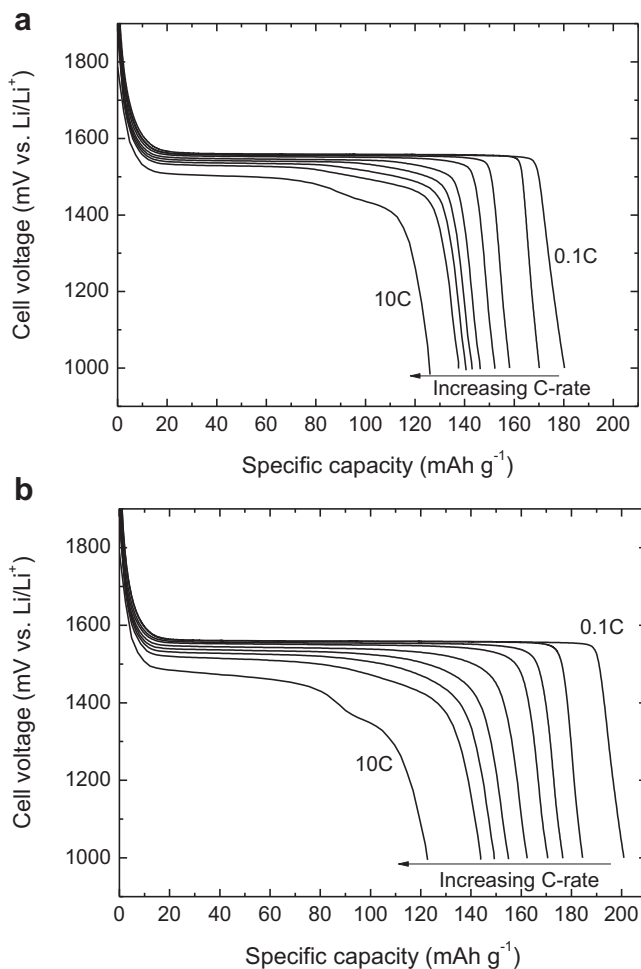


Fig. 3. Discharge curves of the $\text{Li}_4\text{Ti}_5\text{O}_{12}$ electrodes with a) the PVDF and b) Acryl S020 binder measured with C-rates of 0.1; 0.2; 0.5; 1; 2; 3; 4; 5 and 10.

electrode with Acryl S020 and 130 mAh g^{-1} for the electrode with PVDF) are stable for the first 200 cycles and equal within the experimental error originating from the low masses of the electrodes. Also current efficiencies (not shown) are stable and high, higher than 99.8%, which is a typical value for lithium ion batteries, indicating that no unwanted side reactions occur on the studied electrodes. Moreover, energy efficiencies of the $\text{Li}_4\text{Ti}_5\text{O}_{12}$ cells are high, 94.5% and 96.0% for the electrodes with the Acryl S020 and PVDF binder, respectively, indicating low polarization of the electrodes during charging and discharging for the whole period of 200 cycles. Lower energy efficiency of the Acryl S020 containing electrode can be explained by the thicknesses of the electrodes as this one is slightly thicker than the PVDF based electrode resulting in higher internal resistance causing higher irreversible joule heating.

Encouraged by the promising results obtained with the lithium titanate electrodes prepared using aqueous process and the Acryl S020 binder at the laboratory scale, pilot scale preparation of the electrode slurries and utilization of gravure printing and slot die coating methods have been investigated. These techniques resulted in electrodes with highly different masses of the electrode materials on aluminium foil, 0.7 mg cm^{-2} and 3.8 mg cm^{-2} with the gravure and slot die method, respectively. Fig. 6 shows that both these methods produced electrodes with a capacity (140 – 150 mAh g^{-1} and about 150 mAh g^{-1} for the slot-die and gravure electrodes, respectively) which is comparable to that of the laboratory-scale electrode in Fig. 5 (145 mAh g^{-1} with an electrode

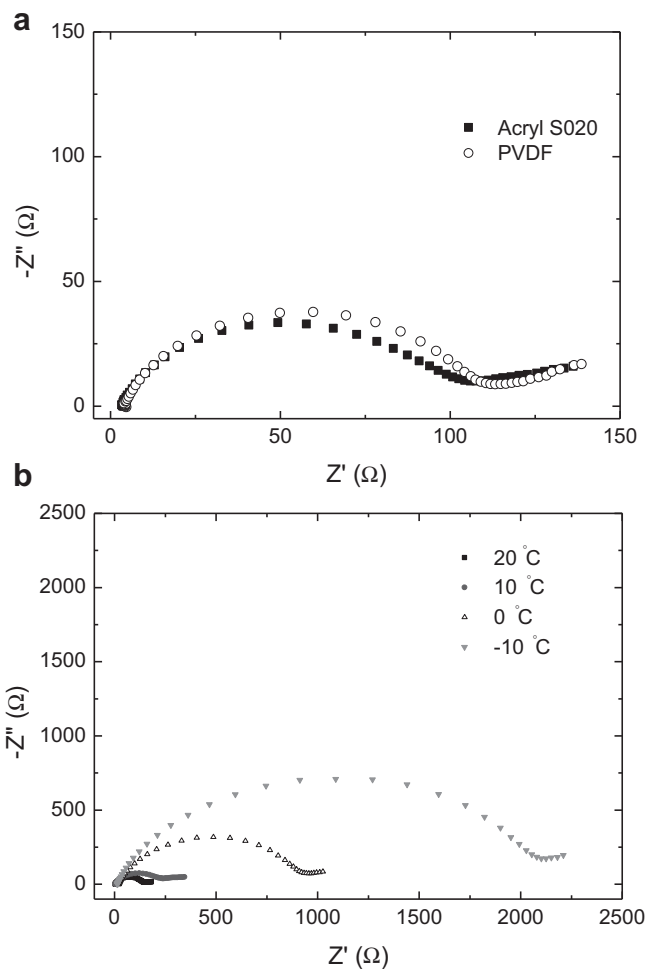


Fig. 4. a) Impedance of the half cells of the $\text{Li}_4\text{Ti}_5\text{O}_{12}$ electrodes with the Acryl S020 and PVDF binders at 20°C b) Impedance of the half cell of the $\text{Li}_4\text{Ti}_5\text{O}_{12}$ electrode with the Acryl S020 binder at different temperatures.

mass of 1.5 – 2.5 mg cm^{-2}) but the capacity of the gravure electrode is stable whereas the slot-die electrode show increasing capacity with time. The initial lower capacity of the thicker slot-die electrode results from higher resistances and mass transport problems

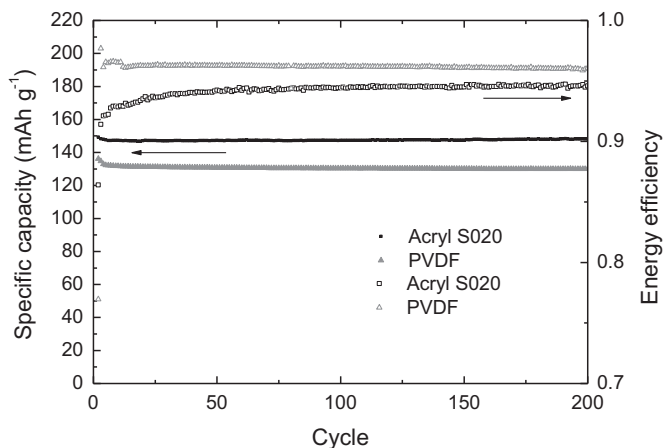


Fig. 5. Specific capacities (full symbols) and energy efficiencies (open symbols) of the half cells with lithium titanate electrode fabricated using the Acryl S020 (black symbols) and PVDF (grey symbols) binders at 1 C rate for 200 cycles.

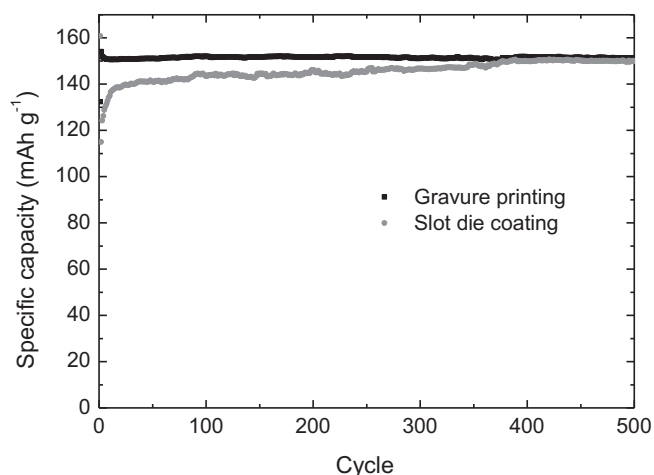


Fig. 6. Specific capacity for 500 cycles at 1 C rate for the $\text{Li}_4\text{Ti}_5\text{O}_{12}$ half cells. Electrodes have been fabricated with an aqueous process using the Acryl S020 binder and printed with a gravure method (black) and coated by a slot-die (grey).

caused by longer pathways for electron and lithium ion transfer, mainly due to longer distances between the current collector and the electrode surface facing the electrolyte. The increase of the capacity, on the other hand, is most likely due to morphological changes induced by the cycling. Unfortunately, despite of the observed high capacity, the extremely thin electrode obtained by the gravure method might not be applicable to practical lithium ion batteries because of low energy densities. However, both aqueous based pilot scale methods can be used to produce durable electrodes withstanding at least 500 cycles without decrease in the capacity, as shown in Fig. 6.

4. Conclusions

Replacing the commonly used, organic solvent based Li-ion battery electrode fabrication processes with the ones utilizing water would help to decrease the price of the lithium ion batteries as well as to reduce the technology's environmental burden. This paper has demonstrated an aqueous fabrication process of an active and stable $\text{Li}_4\text{Ti}_5\text{O}_{12}$ electrode using Acryl S020 as a binder: this type of electrode shows a cycle life of at least 500 cycles and according to electrochemical characterization, its performance is well comparable with the commonly used electrodes with a PVDF binder and organic solvent based preparation process. Furthermore, the electrode shows good capacity retention and the results obtained for it at sub-zero temperatures indicate that the $\text{Li}_4\text{Ti}_5\text{O}_{12}$ electrode with the Acryl S020 binder is also a suitable composition to be used at lower temperatures as the decrease in temperature does not alter the chemistry and stability of the electrodes.

Moreover, the studies with the pilot scale methods (gravure printing and slot die coating) indicate that the aqueous electrode fabrication process introduced here could also be suitable for a larger scale production. As Acryl S020 is an inexpensive binder material which is easy to process, dries fast and is commercially available, this process is a promising alternative for traditional organic solvent based methods for fabricating electrodes of $\text{Li}_4\text{Ti}_5\text{O}_{12}$.

Acknowledgement

Tekes(No. 3087/31/08) and Academy of Finland (No. 126528, 122985 and 255562) are thanked for financial support. Dr. Yliniemi acknowledges also The Finnish Foundation for Technology Promotion for the funding supporting her visiting researcher period in SPECIFIC, Swansea University (UK) and the EPSRC and TSB are thanked for funding the SPECIFIC Innovation and Knowledge Centre. Moreover, Mr. Otto Mustonen is thanked for drawing the $\text{Li}_4\text{Ti}_5\text{O}_{12}$ structure [22,23].

References

- [1] H. Maleki, G. Deng, I. Kerzhner-Haller, A. Anani, J.N. Howard, J. Electrochem. Soc. 147 (2000) 4470–4475.
- [2] C.-C. Li, J.-T. Lee, X.-W. Peng, J. Electrochem. Soc. 153 (2006) A809–A815.
- [3] C.-C. Li, J.-T. Lee, C.-Y. Lo, M.-S. Wu, Electrochem. Solid State Lett. 8 (2005) A509–A512.
- [4] J.-T. Lee, Y.-J. Chua, X.-W. Peng, F.-M. Wang, C.-R. Yang, C.-C. Li, J. Power Sources 173 (2007) 985–989.
- [5] J.H. Lee, J.S. Kim, Y.C. Kim, D.S. Zang, U. Paik, Ultramicroscopy 108 (2008) 1256–1259.
- [6] W. Porcher, B. Lestriez, S. Jouanneau, D. Guyomard, J. Power Sources 195 (2010) 2835–2843.
- [7] S.F. Lux, F. Schappacher, A. Balducci, S. Passerini, M. Winter, J. Electrochem. Soc. 157 (2010) A320–A325.
- [8] J. Chong, S. Xun, H. Zheng, X. Song, G. Liu, P. Ridgway, J.Q. Wang, V.S. Battaglia, J. Power Sources 196 (2011) 7707–7714.
- [9] Z.P. Cai, Y. Liang, W.S. Li, L.D. Xing, Y.H. Liao, J. Power Sources 189 (2009) 547–551.
- [10] G.T. Kim, S.S. Jeong, M. Joost, E. Rocca, M. Winter, S. Passerini, A. Balducci, J. Power Sources 196 (2011) 2187–2194.
- [11] H. Buqa, M. Holsapfel, F. Krumeich, C. Veit, P. Novak, J. Power Sources 161 (2006) 617–622.
- [12] J.H. Lee, S. Lee, U. Paik, Y.M. Choi, J. Power Sources 147 (2005) 249–255.
- [13] J.H. Lee, U. Paik, V.A. Hackley, Y.M. Choi, J. Electrochem. Soc. 152 (2005) A1763–A1769.
- [14] T. Ohzuku, Y. Iwakowshi, K. Sawai, J. Electrochem. Soc. 140 (1993) 2490–2498.
- [15] J.H. Lee, U. Paik, V.A. Hackley, Y.M. Choi, J. Power Sources 161 (2006) 612–616.
- [16] J. Drogenik, M. Gaberscek, R. Dominko, F.W. Poulsen, M. Mogensen, S. Pejovnik, J. Jamnik, Electrochim. Acta 48 (2003) 883–889.
- [17] S. Räsänen, M. Lehtimäki, T. Aho, K. Vuorilehto, M. Karppinen, Solid State Ionics 211 (2012) 65–68.
- [18] S. Räsänen, M. Karppinen, Thermochim. Acta 547 (2012) 126–129.
- [19] C.H. Chen, J. Liu, K. Amine, J. Power Sources 96 (2001) 321–328.
- [20] N. Schweikert, H. Hahn, S. Indris, Phys. Chem. Chem. Phys. 13 (2011) 6234–6240.
- [21] D.P. Abraham, J.R. Heaton, S.-H. Kang, D.W. Dees, A.N. Jansen, J. Electrochem. Soc. 155 (2008) A41–A47.
- [22] K. Momma, F. Izumi, J. Appl. Cryst. 44 (2011) 1272–1276.
- [23] I.A. Leonidov, O.N. Leonidova, L.A. Perelyaeva, R.F. Samigullina, S.A. Kovyazina, M.V. Patrakeev, Phys. Solid State 45 (2003) 2183–2188.